Dig Dis Sci (2012) 57:1227–1237
DOI 10.1007/s10620-012-2031-9

ORIGINAL ARTICLE

The N-Terminal Fragment of Chromogranin A, Vasostatin-1 Protects Mice From Acute or Chronic Colitis Upon Oral Administration

Cristiano Rumio · Giuseppina F. Dusio · Barbara Colombo · Anna Gasparri · Diego Cardani · Fabrizio Marcucci · Angelo Corti

Received: 23 June 2011 / Accepted: 4 January 2012 / Published online: 26 January 2012

Abstract
Background Vasostatin-1 (VS-1), the N-terminal fragment of chromogranin A (CgA), decreases the permeability of endothelial cells in vitro and in vivo.
Aims Here, we investigated whether a similar effect could be observed also on intestinal epithelial cells (IECs) in vitro and whether VS-1 could have favorable effects on animal models of acute or chronic colitis, which are characterized by increased permeability of the intestinal epithelium.
Methods In vitro, VS-1 was tested on IEC monolayers showing increased permeability, on mechanically injured IEC monolayers, and on the production of the chemokine IL-8/KC by lipopolysaccharide (LPS)-stimulated IECs. In vivo, VS-1 was tested in animal models of dextran sodium salt (DSS)-induced acute or chronic colitis.
Results In vitro, VS-1 inhibited increased permeability of IECs induced by interferon-γ and tumor necrosis factor-α. Moreover, VS-1 promoted healing of mechanically injured IEC monolayers, most likely through stimulation of cell migration, rather than cell proliferation. Eventually, VS-1 inhibited LPS-induced production of IL-8. In vivo, VS-1 exerted protective effects in animal models of acute or chronic colitis upon oral, but not systemic administration.
Conclusions VS-1 is therapeutically active in animal models of acute or chronic, DSS-induced colitis. The mechanisms underlying this effect are likely to be multiple, and may include inhibition of enhanced intestinal permeability, repair of injured intestinal mucosae, and inhibition of the production of IL-8/KC and possibly other inflammatory cytokines.

Keywords Chromogranin A · Vasostatin-1 · Intestinal epithelial cells · Inflammatory bowel diseases

C. Rumio · G. F. Dusio · D. Cardani
iMIL—Italian Mucosal Immunity Laboratory, Dipartimento di Morfologia Umana e Scienze Biomediche "Città Studi", Università degli Studi di Milano, via Mangiagalli, 31-20133 Milano, Italy

B. Colombo · A. Gasparri · A. Corti
Division of Molecular Oncology, San Raffaele Scientific Institute, 20132 Milan, Italy

F. Marcucci (✉)
Centro Nazionale di Epidemiologia, Sorveglianza e Promozione della Salute (CNESPS), Istituto Superiore di Sanità (ISS), Via Giano della Bella 34, 00162 Roma, Italy
e-mail: fabmarcu@tin.it

F. Marcucci
Hepatology Association of Calabria, vico Cartisano I°, 89134 Pellaro Reggio Calabria, Italy

Introduction

Crohn's disease and ulcerative colitis, collectively referred to as inflammatory bowel diseases (IBDs), are characterized by chronic inflammation of the intestinal mucosal tissue, and are accompanied by symptoms like abdominal pain, severe diarrhea, rectal bleeding and wasting [1]. It has been proposed that three main features should be present for IBDs to occur: (1) a genetically susceptible mucosal immune system; (2) antigens or pro-inflammatory substances which reach the gut and can trigger the native and adaptive immune system; and (3) increased intestinal permeability with alteration of the gut barrier function, which allows antigens to contact the immune system [2, 3].

These features are tightly linked and impact on each other. Thus, in patients with Crohn's disease, altered barrier function and increased intestinal permeability are present even before insurgence of overt disease [4–8]. Increased intestinal permeability, on the other hand, leads to excessive or inappropriate exposure of the mucosal immune system to intestinal microflora with consequent inflammation and appearance of pathological and clinical symptoms via innate and/or adaptive immune responses. Contribution of microflora is crucial for the pathogenesis of IBDs; in murine models, inflammation fails to develop if susceptible animals are raised in a germ-free environment [9–11].

The role of inflammation and inflammatory cytokines, like tumor necrosis factor (TNF)-α, in the establishment of pathologic and clinical signs of IBDs is best demonstrated by the therapeutic efficacy of anti-TNF-α compounds, which are now a mainstay in the treatment of IBDs [12–15]. One of the effects of inflammatory cytokines like TNF-α and interferon (IFN)-γ is to increase intestinal permeability, mainly through the paracellular route [16–18]. This suggests the existence of a positive feedback loop between enhanced intestinal permeability and increased production of inflammatory cytokines.

Inflammatory cytokines may also cause direct damage to the intestinal epithelium. Pro-apoptotic effects of these cytokines can lead to the formation of refractory ulcers in the intestine [19, 20]. Apoptosis of intestinal epithelial cells (IECs) and subsequent ulceration of the mucosa may amplify defects in intestinal permeability, thereby further adding to the positive feedback loop between increased intestinal permeability, enhanced production of inflammatory cytokines, and damaged intestinal epithelium.

Previous studies showed that vasostatin-1 (VS-1), the N-terminal fragment encompassing amino acids 1–78 of chromogranin A (CgA), could inhibit vascular leakage by decreasing the permeability of endothelial cells [21–24]. In particular, these studies demonstrated that VS-1 can protect the endothelial barrier integrity against the effects of TNF-α and VEGF. These findings, together with preliminary results obtained in vitro, in permeability assays performed with IECs, led us to hypothesize that VS-1 may also affect the barrier function of IECs. For this purpose, we investigated the effect of VS-1 on the barrier function of IECs and other in vitro assays, as well as in vivo using murine models of IBDs. The results show that VS-1 inhibits permeability enhancement of IEC monolayers induced by inflammatory cytokines, promotes healing of mechanically injured IEC monolayers and suppresses LPS-induced production of the inflammatory chemokine IL-8/KC. Eventually, VS-1 was shown to be therapeutically active upon oral administration of VS-1 to mice with acute or chronic colitis induced by dextran sodium salt (DSS).

Methods

Cell Lines

T84 and Caco-2 human colorectal carcinoma epithelial cells were obtained from the American Type Culture Collection (Manassas, VA). T84 cells were maintained in Dulbecco's modified Eagle's medium (DMEM, Invitrogen)/Ham's F-12 (1:1) supplemented with 10% fetal calf serum, penicillin G sodium (100 U/ml), and streptomycin sulfate (100 μg/ml) (Sigma-Aldrich). Caco-2 cells were maintained in DMEM with L-glutamine, supplemented with 10% fetal bovine serum (FBS), 200 U/ml penicillin and 200 μg/ml streptomycin, 1 mmol/l sodium pyruvate, and 1% non-essential amino acids (all from Sigma-Aldrich). Cells were grown at 37°C in a 5% CO_2 humidified atmosphere.

Preparation of VS-1

Recombinant human Ser-Thr-Ala-$CgA_{1–78}$ (VS-1) was produced as previously described [25].

Induction of Enhanced Permeability of IEC Monolayers

Caco-2 cells were grown as monolayers on collagen-coated polycarbonate membrane Transwell supports with 0.33 cm^2 area (Corning-Costar, Acton, MA, USA) and used 17–20 days after confluence. Some Caco-2 monolayers were cultured for 24 h in medium alone. Other Caco-2 monolayers were incubated with IFN-γ (10 ng/ml) for 16 h and also with TNF-α (2.5 ng/ml) for an additional 8 h, for an overall 24 h (both from R&D System, Minneapolis, USA). These cytokines enhance paracellular permeability by inducing degradation of tight junction proteins [18, 26]. Cytokines were added to the basal chamber without manipulating the apical medium. Still other monolayers were incubated during the 24 h by also adding VS-1 to the apical medium.

Alteration of the permeability of Caco-2 IEC monolayers was tested by measuring the flux of fluorescein isothiocaynate dextran (FD3, molecular weight 3 kDa, Molecular Probes, Eugene, OR, USA) [27]. Monolayers were washed free of media and equilibrated with Hank's balanced salt solution (HBSS, Sigma) at 37°C prior to addition of the fluorescent tracer. Apical medium was removed and 250 μl of FD-3, 1 mg/ml diluted in HBSS, were added to the apical chamber. Then, 50 μl samples were removed from the apical and basal chambers 30 and 120 min after the end of the different treatments, and fluorescence intensity (excitation, 485 nm; emission, 530 nm) was measured on a fluorescent plate reader (Citofluor™ 2300, Millipore Inc. Bedford, MA, USA).

Tracer concentrations were determined from standard curves generated by serial dilutions of known concentrations of FD-3 in HBSS. All data were normalized for background fluorescence by subtraction of fluorescence intensity of samples collected from monolayers incubated with buffer alone.

Healing of Mechanically Injured IEC Monolayers

Monolayers of Caco-2 cells were maintained in medium supplemented with 0.1% FBS for 18 h and subsequently the monolayers were mechanically injured with a 10-µl pipette tip and washed with phosphate-buffered saline (PBS). Caco-2 monolayers were incubated for 24 h with medium supplemented with 0.1% FBS, medium supplemented with 0.1% FBS and VS-1, or medium supplemented with 10% FBS. Cultures were examined and images acquired with a digital camera after 2, 4, 6 and 24 h incubation [28, 29]. Damage repair was calculated as percentage of denuded area covered by migrating cells.

To determine cell densities, an 3-(4,5-dimethylthiazol-2-yl)-2,5-diphenyltetrazolium bromide stock solution (5 mg/ml distilled water) was filter-sterilized. To start the color reaction, the stock solution was added for 3 h to cell cultures growing in 96-well plates (final concentration, 0.5 mg/ml). Then, 100 µl of HCl 0.1 N in isopropanol were added to each well and cells were suspended. The OD was measured with a spectrophotometer (Cytofluor 2300, Millipore Inc., Bedford, MA) at 550 nm, with 690 nm as a reference read-out. A blank with propanol alone was measured and subtracted from all values.

Interleukin-8 (IL-8) Production by IECs and Determination of IL-8 and KC

T84 cells were cultured for 18 h in complete medium and stimulated with *Salmonella enterica* LPS (1 µg/ml) (Sigma Aldrich). Supernatants were collected at the end of treatment and stored at −80°C. IL-8 was measured using enzyme-linked immunosorbent assay (ELISA) kits from Endogen (Woburn, MA) and carried out according to the manufacturer's instructions. The mouse equivalent of IL-8, KC, was measured in supernatants of organ cultures and murine plasma samples using ELISA kits from R & D Systems (Minneapolis, MN) and carried out according to the manufacturer's instructions.

VS-1 ELISAs

VS-1 was measured using three sandwich ELISAs based on anti-VS-1 mAbs directed against different epitopes [30, 31]. The following antibodies [32, 33] were used: mAb 7D1 (recognizing an epitope encompassing amino acids 34–46 of CgA), mAb 5A8 (amino acids 54–57), and mAb B4E11 (amino acids 68–71). In two ELISA systems, mAb 5A8 was used in the capture step followed by biotinylated mAb 7D1 or biotinylated mAb B4E11 in the detection step. The third assay was based on the use of mAb B4E11 in the capture step and of biotinylated mAb 7D1 in the detection step. Bound antibodies were detected with a peroxidase-streptavidin conjugate. Each assay was calibrated using recombinant VS-1 standard solutions.

Induction of Acute or Chronic Colitis in Mice and Evaluation of Clinical Signs

C57BL/6 female mice were purchased from Charles River, Italy (Calco, Italy). They were housed under specific pathogen-free conditions, maintained at constant temperature and humidity, with food and water given ad libitum, and used at 8–12 weeks of age. Mice were randomly distributed in groups of ten animals each.

To induce acute colitis, mice weighting 20–22 g received 2% DSS (40 kDa, MP Biomedicals, Irvine, CA, USA) ad libitum in filter-purified drinking water for 7 days [34]. Some groups of mice also received VS-1 in PBS from day 4 to day 7. VS-1 was administrated with a sterile stomach tube. Another group of mice received PBS alone.

To induce chronic colitis, mice received four cycles of DSS 2%. For each cycle they received 2% DSS in filter-purified drinking water for 7 days, followed by a 14-day interval with water alone. Treatments with VS-1 were started 10 days after the last DSS cycle, 5 times/week for 3 consecutive weeks (as reported in Table 1).

All groups were sacrificed after the last week of VS-1 administration. A schematic representation of this treatment protocol is given in Table 1.

Table 1 Chronic colitis and treatment with vasostatin-1 (VS-1): induction protocol

Treatment	DSS	H_2O	DSS	H_2O	DSS	H_2O	VS-1[b] 5×/week for 3 weeks
No. of days[a]	7	14	7	14	7	10	15

[a] Number of days indicates number days of administration of water with or without dextran sodium salt (DSS). After the last DSS cycle, VS-1 was administrated 5 times/week for 3 weeks

[b] VS-1 was administrated at the following doses: 0.1, 0.3, 1, 3, 30 µg/mouse/day

Table 2 Scoring system for inflammation-associated histological changes in the colon

Score	Histologic changes
0	No evidence of inflammation
1	Low level of inflammation with scattered infiltrating mononuclear cells
2	Moderate inflammation with multiple foci
3	High level of inflammation with increased vascular density and marked wall thickening
4	Maximal severity of inflammation with transmural leukocyte infiltration and loss of globet cells

Colitis was scored daily using standard parameters. Body weight of mice was registered daily at 5:00 PM. For histological evaluation of colitis severity, murine colon specimen were fixed in 10% neutral-buffered formalin for 4 h, embedded in paraffin, sectioned at 4 μm and collected on silanized slides.

For histopathological analysis, hematoxylin-eosin-stained sections of samples of the distal colon were used. Samples were observed with a Nikon Eclipse 80i microscope equipped with a digital Nikon DS-L1 camera. To quantify/evaluate acute or chronic colitis-associated histological alterations in the colon we used the scoring system detailed in Table 2.

In order to measure colon permeability, organ segments were mounted between the two chambers of an Ussing System (0.125 cm^2 opening). Two calomel voltage-sensitive electrodes and two Ag–AgCl current-passing electrodes (EVC-4000 World Precision Instrument Inc., Sarasota, FL) were connected to the Ussing chamber via agar bridges. Both the mucosal and serosal sides of the chamber were connected to sterilized circulating reservoirs containing 10 ml of oxygenated Krebs buffer (115 mM NaCl, 8 mM KCl, 1.25 mM $CaCl_2$, 1.2 mM $MgCl_2$, 2 mM KH_2PO_4, and 225 mM $NaHCO_3$; pH 7.35) (all reagents purchased from Merk). The buffers were maintained at 37°C by a heated water jacket and circulated by a gas lift column of 95% oxygen/5% CO2. Glucose (5.5 mM) was added to the serosal and mucosal sides. Colonic membranes were mounted in the Ussing chamber, and the system was allowed to stabilize for 20 min in order to test its functionality and the integrity of the colonic mucosal membrane. Trans-epithelial electrical potential difference in millivolts across the mucosal membrane was measured directly, while the trans-membrane resistance was calculated indirectly as ohms × cm^2, using Ohm's law.

For organotypic cultures, the colon was excised, opened, and cut transversely into three parts. Each segment was washed in cold PBS containing penicillin, streptomycin, and amphotericin B (the last purchased from Cambrex; BioWhittaker, Walkersville, MD) and incubated 24 h in serum-free RPMI 1640 medium containing 0.1% penicillin, streptomycin, and amphotericin B at 37°C in 5% CO_2. After 2 h, supernatants were collected, centrifuged, and stored at −80°C for determination of KC.

Statistical Analysis

Student's *t* test (paired two-tailed) and GraphPad Prism software (GraphPad Prism Software Inc., San Diego, CA, USA) were used for comparisons between groups.

Ethical Considerations

Animal studies were performed in accordance with the guidelines on the use of laboratory animals set by the Human Morphology and Biomedical Sciences Department "Città Studi" of the Università degli Studi di Milano.

Results

VS-1 Inhibits the Cytokine-Induced Increase of Permability of IEC Monolayers

In vitro studies have shown that VS-1 inhibits TNF-α-induced endothelial barrier dysfunction [23, 24]. These observations led us to test whether VS-1 could have similar effects on cytokine-induced impairment of the permeability of IECs. Addition of INF-γ (10 ng/ml) and TNF-α (25 ng/ml) for 24 h to a Caco-2 cell monolayer led to a 25-fold increase of the flux of FD-3—from 11 ± 7.5 to 278 ± 28 pmol/cm^2/h. Addition of VS-1 (0.1, 1, 3 and 10 μg/ml) during the incubation with INF-γ and TNF-α prevented this increase of permeability (Fig. 1a). A dose–response effect was observed, with 1, 3 and 10 μg/ml of VS-1 almost completely or completely preventing the cytokine-induced increase of permeability, and with 0.1 μg/ml leading to a 50% (IC_{50}) reduction of the FD-3 flux (134.82 ± 6.232 pmol/cm^2/h). Addition of the same doses of VS-1, in the absence of INF-γ and TNF-α, did not modify the permeability of Caco-2 monolayers (data not shown).

VS-1 Inhibits LPS-Induced IL-8 Production

We tested the effect of VS-1 on LPS-induced IL-8 production, an inflammatory chemokine that has been shown to be elevated in patients with IBDs, and suggested to play a role in the disease pathogenesis [35–37]. For this purpose, T-84 IECs (Fig. 1b) were stimulated with *Salmonella enterica* LPS in the absence or presence of 3 μg/ml VS-1. LPS-stimulated T-84 cells produced high levels of IL-8. In

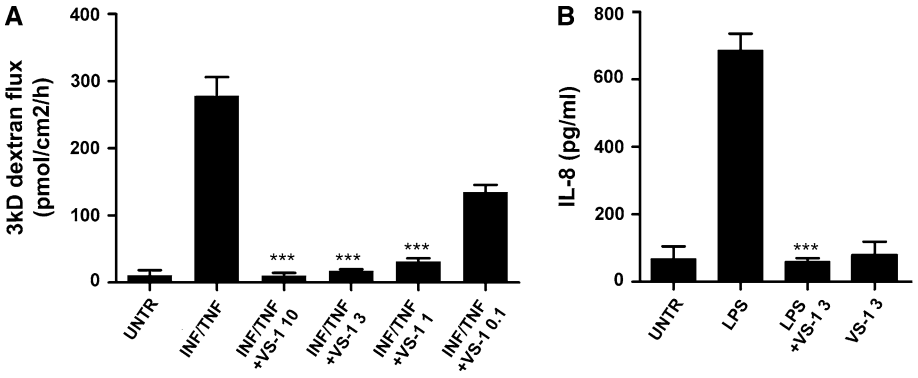

Fig. 1 **a** Vasostatin-1 (VS-1) inhibits interferon-γ (IFN-γ)/tumor necrosis factor-α (TNF-α)-induced increase of permeability of intestinal epithelial cells. Monolayers were assayed for permeability to 3 kD fluorescein isothiocyanate-dextran (FD-3). *UNTR* untreated cells; *IFN/TNF* cells treated with IFN-γ and TNF-α; *IFN/TNF VS-1 10* cells treated with IFN-γ, TNF-α and VS-1 (10 μg/ml); *IFN/TNF VS-1 3* cells treated with IFN-γ, TNF-α and VS-1 (3 μg/ml); *IFN/TNF VS-1 1* cells treated with IFN-γ, TNF-α and VS-1 (1 μg/ml); *IFN/TNF VS-1 0.1* cells treated with IFN-γ, TNF-α and VS-1 (0.1 μg/ml). $IC_{50} = 1$ μg/ml. Data are the mean ± standard deviation (SD) of three replicates assayed in one experiment. ***$P < 0.0001$ versus INF/TNF. **b** Vasostatin-1 (VS-1) inhibits lipopolysaccharide (LPS)-induced interleukin-8 (IL-8) production by T-84 cells. VS-1 was used at 3 μg/ml. ***$P < 0.0001$ versus LPS. *UNTR* untreated cells; *LPS* cells treated with LPS alone; *LPS VS-1* cells treated with LPS and VS-1 (3 μg/ml); *VS-1 3* cells treated with VS-1 (3 μg/ml) alone

the presence of VS-1, however, LPS-induced IL-8 production was strongly inhibited. Addition of the same doses of VS-1, in the absence of LPS, did not modify IL-8 levels.

VS-1 Promotes Healing of Mechanically Injured IEC Monolayers In Vitro

To investigate the effect of VS-1 on damaged IEC monolayers, Caco-2 cell monolayers were injured with a pipette tip, and then cultured in 0.1% FBS-supplemented medium, 0.1% FBS-supplemented medium plus VS-1 (3 μg/ml) or 10% FBS-supplemented medium. Cells treated with VS-1 showed a marked decrease of the percentage of denuded area compared to cells incubated with 0.1% FBS-supplemented medium alone (Fig. 2a). The degree of damage repair was similar to that obtained upon incubation with 10% FBS-supplemented medium. Figure 2b, however, shows that the mechanism underlying accelerated healing of damaged IECs was different for cells incubated with 0.1% FBS-supplemented medium and VS-1 compared to cells incubated with 10% FBS-supplemented medium. In fact, cells cultured in 10% FBS-supplemented medium proliferated much more rapidly than cells in 0.1% FBS-supplemented medium without or with 3 μg/ml VS-1. This result suggests that VS-1 leads to coverage of the denuded area through stimulation of cell migration, rather than cell proliferation.

VS-1 Affords Protection in Murine Models of Acute and Chronic Colitis

VS-1 was first tested in a model of acute colitis. Four days after induction of acute colitis with DSS, animals were

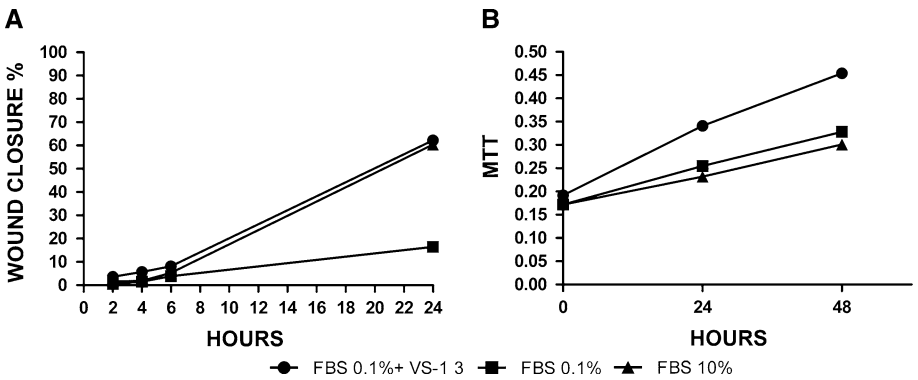

Fig. 2 **a** Vasostatin-1 (VS-1) accelerates healing of a mechanically injured monolayer of Caco-2 cells. **a** Repair of mechanically injured monolayers of Caco-2 cells. **b** MTT (3-(4,5-dimethylthiazol-2-yl)-2,5-diphenyltetrazolium bromide) proliferation assay of Caco-2 cells after mechanical injury. *FBS 0.1%* control cells incubated with 0.1% fetal bovine serum; *FBS 0.1% VS-1 3* cells incubated with 0.1% FBS-supplemented medium and VS-1 (3 μg/ml); *FBS 10%* cells incubated with 10% FBS-supplemented medium

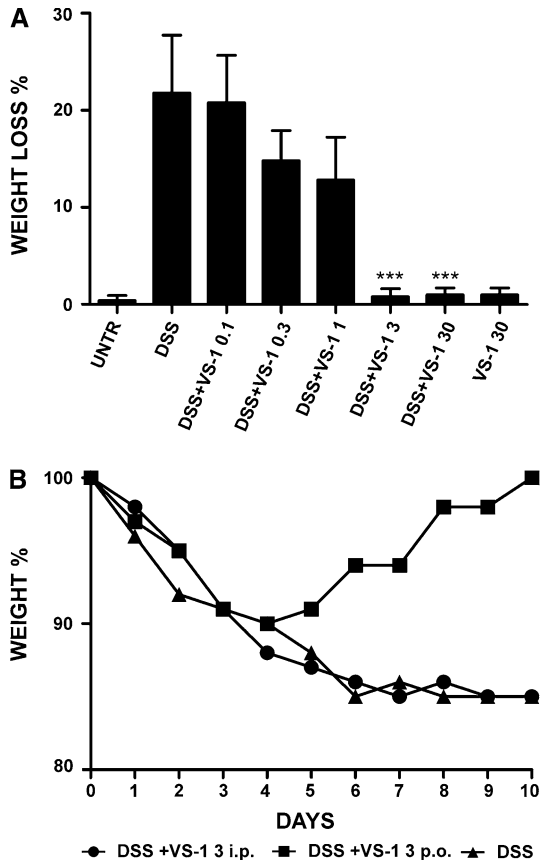

Fig. 3 **a** Orally administered Vasostatin-1 (VS-1) prevents weight loss in dextran sodium salt (DSS)-treated mice. *UNTR* untreated animals; *DSS + VS-1 0.1* mice treated with DSS and 0.1 μg VS-1/mouse; *DSS + VS-1 0.3* mice treated with DSS and 0.3 μg VS-1/mouse; *DSS + VS-1 1* mice treated with DSS and 1 μg VS-1/mouse; *DSS + VS-1 3* mice treated with DSS and 3 μg VS-1/mouse; *DSS + VS-1 30* mice treated with DSS and 30 μg VS-1/mouse; *VS-1 30* mice treated with VS-1 (30 μg/mouse) alone. $IC_{50} = 1.3$ μg/mouse. Data represent the mean ± standard deviation (SD) of 10 mice/group. ***$P < 0.0001$ versus DSS. **b** Vasostatin-1 (VS-1) prevents weight loss in dextran sodium salt (DSS)-treated mice only when administered by oral, but not intraperitoneal route. *Black triangles* animals treated with DSS alone; *black squares* animals treated with DSS and 3 μg/mouse/day of VS-1 administered by oral route; *black dots* animals treated with DSS and 3 μg/mouse/day of VS-1 administered by intraperitoneal route

treated orally with different doses of VS-1. As shown in Fig. 3a, VS-1 induced a dose-dependent recovery of DSS-induced weight loss with an IC_{50} value of ~1.3 μg/day (as calculated by extrapolation from the values indicated in Fig. 3a). At a concentration of 0.1 μg/day VS-1 was ineffective. In this and the other experiments shown, VS-1 alone was inactive on all parameters studied.

In another experiment we tested whether VS-1 could also protect from acute colitis upon systemic administration. For this purpose, DSS-treated animals were administered 3 μg VS-1 either by oral or intraperitoneal route. As can be seen from Fig. 3b, in contrast to oral administration, intraperitoneal administration of VS-1 was ineffective in protecting animals from DSS-induced weight loss.

Next, we tested the effect of VS-1 on alteration of the mucosal barrier induced by DSS which is directly toxic for IECs and damages the mucosal barrier. It has already been demonstrated that increased colon permeability is a necessary step in the development of DSS-induced colitis [38, 39]. As expected, DSS-treated mice showed greatly decreased transmembrane resistance compared to the control group (Table 3). On the other hand, in mice treated with DSS and 3 or 30 μg/kg of orally administered VS-1, transmembrane resistance remained similar to untreated mice. These results suggest that VS-1 inhibits DSS-induced increase of colon permeability. One of the hallmarks of DSS-induced intestinal damage is the decreased length of the affected distal colon [34, 39]. Thus, in our experiments, the mean colon length of mice treated with DSS decreased by 32% compared to untreated mice. Also in this case, oral administration of VS-1 preserved colon length of DSS-treated mice at levels similar to control mice (Table 4).

Eventually, we also measured the levels of the inflammatory cytokine KC (mouse equivalent of human IL-8) in the plasma and in full-thickness organ cultures of the colon of animals treated with DSS alone or with DSS and VS-1. Plasma levels of KC were strongly increased in mice with DSS-induced acute colitis, while they were similar to controls in DSS-induced mice that had been treated orally with VS-1 ($IC_{50} \ll 3$ μg/mouse, Fig. 4a). Similarly, KC levels in supernatants from organ cultures of DSS-treated animals were much higher than untreated controls (Fig. 4b). Also in this case, oral administration of VS-1 to DSS-treated mice yielded KC levels similar to control animals.

VS-1 was also tested in a mouse model of DSS-induced chronic colitis. As shown in Table 5, oral administration of VS-1 led to complete inhibition of the reduction of intestinal transmembrane resistance in mice with DSS-induced chronic colitis. The protective activity of VS-1 showed a

Table 3 Intestinal transmembrane resistance in mice treated with dextran sodium salt (DSS) alone or DSS + vasostatin-1 (VS-1) ($n = 3$/group, mean ± SD)

Measurement	Untreated	DSS alone	DSS + 3 μg VS-1/mouse	DSS + 30 μg VS-1/mouse
Resistance in Ωxcm^2	53.4 ± 2.7	25 ± 2.2	49.6 ± 1.52	50.4 ± 1.52

Table 4 Colon length in mice treated with dextran sodium salt (DSS) alone or DSS + vasostatin-1 (VS-1) (n = 3/group, mean ± SD)

Measurement	Untreated	DSS alone	DSS + 3 μg VS-1/mouse	DSS + 30 μg VS-1/mouse
Colon length (cm)	8.3 ± 0.7	5.5 ± 0.5	7.8 ± 0.4	8.0 ± 0.6

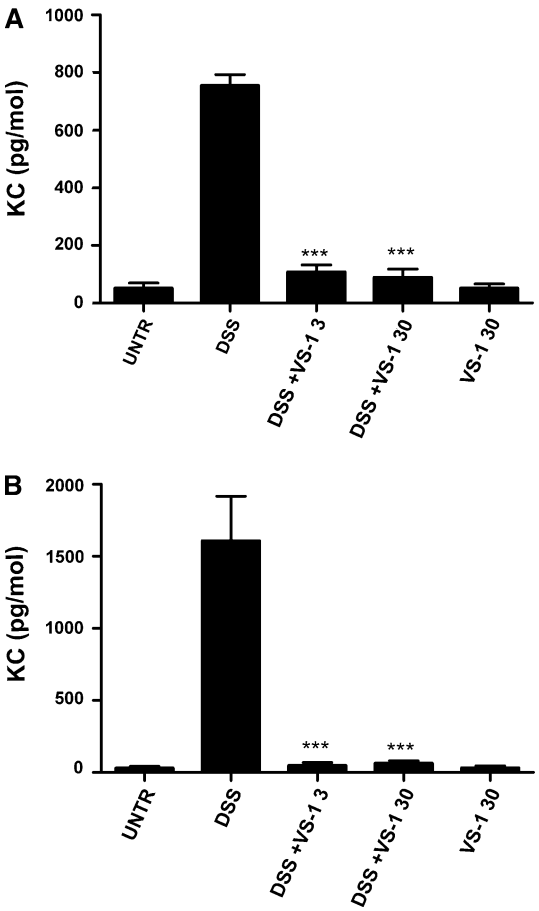

Fig. 4 Orally administered vasostatin-1 (VS-1) inhibits increase of KC levels in dextran sodium salt (DSS)-treated mice. **a** KC levels in plasma. **b** KC levels in organ culture supernatants. *UNTR* untreated mice; *DSS* mice treated with DSS alone; *DSS + VS-1 3* mice treated with DSS and 3 μg VS-1/mouse; *DSS + VS-1 30* mice treated with DSS and 30 μg VS-1/mouse; *VS-1 30* mice treated with VS-1 (30 μg/mouse) alone. ***$P < 0.0001$ versus DSS; estimated IC_{50} value $\ll$ 3 μg/mouse

dose–response effect, since the 1 μg/mouse dose appeared less active than higher doses. Histological examination of colon tissue from DSS-treated mice showed, upon hematoxylin/eosin staining, prominent signs of inflammation with scattered, infiltrating mononuclear cells and thickening of the intestinal wall. On the other hand, very mild signs of inflammation were seen in tissue samples from animals treated with DSS and VS-1 3 μg (Fig. 5).

VS-1 or Fragments Thereof Can Be Recovered from the Gastrointestinal Tract or In Serum After Oral Administration or Intraperitoneal Injection

As already addressed before, the observation that VS-1 was therapeutically active in mouse models of acute or chronic colitis upon oral administration is somehow surprising, since a peptide like VS-1 would be expected to be readily degraded in the harsh environment of the gastrointestinal tract. In order to investigate this aspect, homogenates of the intestine were tested for the presence of VS-1 at different times after oral administration. It was found that 25 min after oral administration of 30 μg VS-1, significant, albeit greatly reduced quantities could be recovered from the homogenates (6–7 ng of VS-1 in the stomach and gut), as shown in Fig. 6a–c. Of note, sandwich ELISAs based on different antibodies against different epitopes detected different levels of VS-1 antigen in tissue extracts. In particular an ELISA assay based on the combination of mAb 5A8 (recognizing CgA epitope 54–57) and mAb 7D1 (34–47) gave higher values compared to the combination of mAb 5A8 and mAb B4E11 (epitope 68–71) indicating that fragments encompassing amino acids 34–57 were more abundant than fragments encompassing amino acids 54–71. To evaluate plasma levels of VS-1 or fragments thereof after systemic delivery, we administered, intraperitoneally, 3 μg of VS-1 to mice and measured VS-1 plasmatic levels using the ELISA based on mAb 5A8 and B4E11. The circulating levels of VS-1 were: (a) undetectable before administration; (b) 1.06 ± 0.15 μg/ml, 1 h after administration; 0.35 ± 0.15 μg/ml, 3 h after administration (Fig. 6d). Given that a mouse has approximately 1.1–1.5 ml of blood, these results suggest that, after 1 h, >1,000 ng of VS-1 are still present in circulation. These results suggest that orally administered VS-1 was degraded more rapidly than systemically delivered VS-1.

Table 5 Intestinal transmembrane resistance in mice treated with dextran sodium salt (DSS) alone or DSS + the indicated doses of vasostatin-1 (VS-1) (n = 3/group, mean ± SD)

Measurement	Untreated	DSS alone	DSS + 1 μg VS-1/mouse	DSS + 3 μg VS-1/mouse	DSS + 15 μg VS-1/mouse
Resistance in Ωxcm^2	49 ± 1.2	34.3 ± 2.1	37.3 ± 2.5	52.7 ± 7.2	50.7 ± 2.1

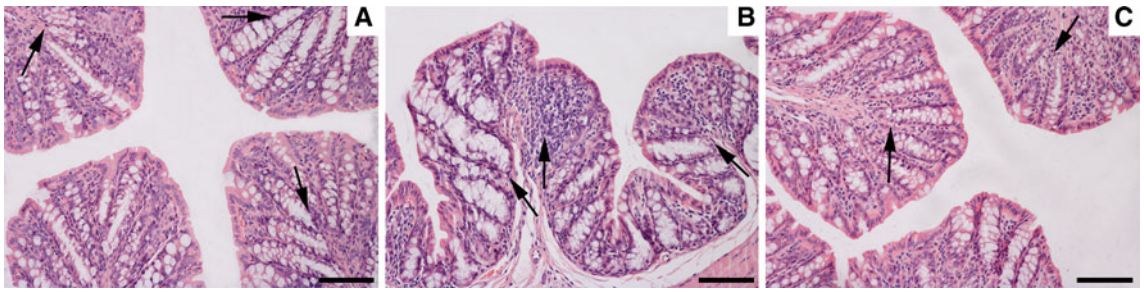

Fig. 5 **a** Representative colon section from mice receiving water alone shows colon crypt with normal morphology (*arrows*). **b** Colon section from DSS-treated mice shows thickening of the wall and infiltration reaching the lamina submucosa (*arrows*). **c** Colon section of VS-1- and DSS-treated mice. Normal morphology with low level of inflammation (*arrows*). *Bars* = 20 μm

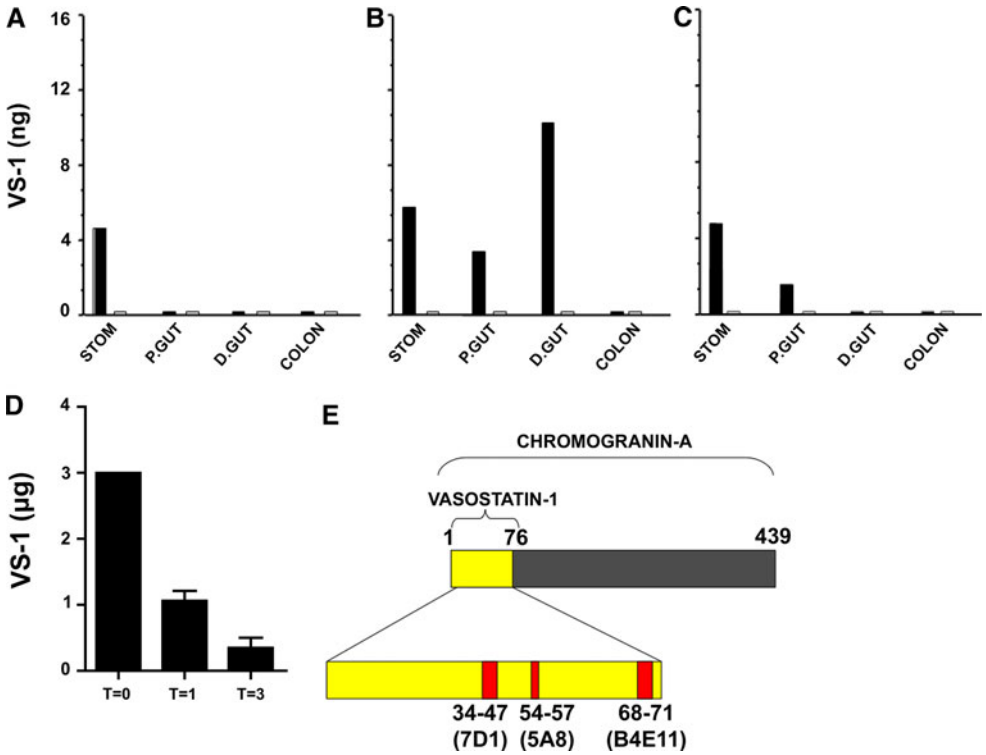

Fig. 6 Vasostatin-1 (VS-1) in tissue extracts from different segments of the gastrointestinal tract after oral administration and in plasma after intraperitoneal injection. VS-1 was administered at 30 μg/mouse (*black bars*) or diluent alone (*white bars*). VS-1 was measured by ELISA with different antibody combinations 25 min after administration. *Stom* stomach; *P.Gut* proximal intestine; *D.Gut* distal intestine. **a** Capture antibody B4E11; detection antibody 7D1. **b** Capture antibody 5A8; detection antibody 7D1. **c** Capture antibody 5A8; detection antibody B4E11. **d** VS-1 was administered at 3 μg/mouse i.p. (T = 0). VS-1 plasma levels were measured 1 h (T = 1) and 3 h (T = 3) after administration in ELISA with mAb5A8 and B4E11 antibodies combination. **e** Schematic representation of VS-1 epitopes detected by mAb 7D1, 5A8 and B4E11

Discussion

CgA is an acidic protein, a member of the granin family, and ubiquitous in secretory cells of the nervous, endocrine and immune systems. CgA was the first granin to be characterized as an acidic protein co-stored and co-released with catecholamine hormones from the bovine adrenal medulla; CgA is also expressed by several other neuroendocrine cells, including cells of the gastroenteropancreatic endocrine system. Intracellular processing of CgA originates several peptides which display a wide range of biological activities [23–40], and VS-1 is one of these peptides. One of the effects of VS-1 is to protect the integrity of endothelial barriers. Thus, VS-1 inhibits TNF-α-induced flux of proteins through endothelial cell monolayers [24] and TNF-α-induced gap formation in arterial

endothelial cells of bovine pulmonary and coronary origin [23]. This protective effect was observed also in vivo, since TNF-α-induced vascular leakage through liver vessels in mice was inhibited by recombinant VS-1 [24]. These observations suggested to us the possibility that VS-1 might also protect the integrity of an epithelial barrier like the intestinal. Enhanced paracellular permeability of the intestinal epithelium is a key event in the pathogenesis of IBDs, and its inhibition is considered a therapeutic goal in IBDs and other diseases [2–8].

In accordance with the possibility that VS-1 might affect permeability of IECs, we observed that recombinant VS-1 inhibited IFN-γ- and TNF-α-increased permeability of Caco-2 cells in a dose-dependent manner.

Subsequently, we tested also whether VS-1 could impact on other events that play important roles in the pathogenesis of IBDs. One of these events is overproduction of inflammatory cytokines [41, 42], and the use of biologicals that inhibit the activity of inflammatory cytokines (mainly TNF-α) are one of the current mainstays in the therapy of IBDs. Indeed, we found that VS-1 inhibited LPS-induced production of IL-8 by intestinal epithelial T-84 cells. IL-8 is an inflammatory cytokine that has been reported to be linked with alteration of the gut flora, a phenomenon thought to play a role in the pathogenesis of IBDs, and Toll-like receptor-4-mediated response to bacterial LPS [43].

Moreover, chronic inflammation of the intestinal epithelium leads to the formation of refractory ulcers in the intestine of IBD patients [20, 44]. This suggested that we should test in vitro whether VS-1 might have effects also on injured epithelial cell monolayers. In fact, we showed that VS-1 could promote healing of mechanically injured monolayers of Caco-2 cells through stimulation of cell migration. These results are consistent with previous observations [34, 45, 46] showing that recombinant VS-1 has an accessible site that induces adhesion and spreading of fibroblasts and smooth muscle cells on solid surfaces.

Altogether, these results show that VS-1 impacts on three in vitro models of some of the main hallmarks of IBDs: enhanced permeability of IECs, enhanced production of pro-inflammatory chemokines, and damaged intestinal epithelium. On this basis it was a logical next step to test whether VS-1 was therapeutically active in animal models of IBDs. For this purpose, VS-1 was administered orally to mice with DSS-induced, acute or chronic colitis. VS-1 had favorable, dose-dependent effects on different parameters that were altered in colitis-affected mice. Thus, it led to recovery from weight loss, inhibited reduced intestinal transmembrane resistance, reduced levels of the inflammatory chemokine KC both in plasma and organ culture, and reduced signs of inflammation in tissue samples from diseased animals. Importantly, VS-1 was active only upon oral but not systemic administration. This suggests that VS-1 becomes available to gastrointestinal epithelial cells only by oral administration or that proteolytic processing in the gastrointestinal tract is necessary for activity.

Moreover, in all our in vivo studies we did not observe overt adverse events upon acute or oral administration of VS-1, including events that might have been predicted on the basis of known pharmacological effects of VS-1, such as on the heart and vascular contractility [23]. However, further studies are necessary to investigate intestinal absorption of VS-1-derived peptides and possible effects on the cardiovascular system upon oral administration of VS-1.

While these results are consistent with the effects that had been observed in vitro, the therapeutic efficacy after oral administration was surprising because one might have expected a 78-residue peptide to be readily degraded in the harsh environment of the stomach and intestinal tract, and not reach the site of its therapeutic action in intact form. Indeed, previous studies have shown that VS-1 can be enzymatically degraded by extracellular proteases such as dipeptidyl peptidase IV (DPP-IV) [47] and trypsin [45]. For this reason we performed experiments aimed at determining the recovery of VS-1 from intestinal homogenates after oral administration and from blood samples after systemic administration. ELISA assays showed that VS-1 is degraded more rapidly in the gastrointestinal tract than in the blood. This result suggests two possible interpretations: first, VS-1 requires only a brief residence time in the gastrointestinal tract in order to induce the relevant biological activities, or second, proteoloytic degradation of VS-1 leads to the generation of a fragment that is the actual inducer of the biological activities. The sharp cleavage of VS-1 also makes it very difficult to speculate on the position of bioactive fragments.

These results, obtained with an orally available peptide (VS-1), while surprising, are not unprecedented. Thus, the orally available octapeptide, zonulin antagonist AT-1001, is being developed for the treatment of celiac and other diseases characterized by increased intestinal permeability. AT-1001 competitively blocks the apical zonulin receptor and prevents the opening of tight junctions [48–50]. AT-1001 has been shown to reduce small intestinal permeability and attenuate colitis in the IL-10 gene-deficient mouse [3]. The orally available AT-1001 has now advanced into phase II clinical trials. These and our results, suggest that orally available peptides may be useful for the treatment of IBDs and, more generally, diseases characterized by enhanced intestinal permeability.

In conclusion, our results show that VS-1 is therapeutically active in animal models of acute and chronic colitis. This is likely the result of different biological activities that

were found in vitro and in vivo: inhibition of intestinal permeability, inhibition of the production of the pro-inflammatory chemokine IL-8, and accelerated healing of injured epithelial cells.

In future work we will assess whether shorter peptides encompassed within the VS-1 sequence may mimic the effects of recombinant VS-1 in the same models. The availability of peptides of reduced size, allowing them to be synthesized chemically, would make them more attractive in view of therapeutic applications.

Acknowledgment This work was supported by the Associazione Italiana per la Ricerca sul Cancro.

Conflict of interest None of the authors has any conflict of interest.

References

1. Podolsky D. Inflammatory bowel disease. *N Engl J Med*. 2007;347:417–429.
2. Arrieta MC, Bistritz L, Meddings JB. Alterations in intestinal permeability. *Gut*. 2006;55:1512–1520.
3. Arrieta MC, Madsen K, Doyle J, Meddings J. Reducing small intestinal permeability attenuates colitis in the IL10 gene-deficient mouse. *Gut*. 2009;58:41–48.
4. D'Inca R, Di Leo V, Corrao G, et al. Intestinal permeability test as a predictor of clinical course in Crohn's disease. *Am J Gastroenterol*. 1999;94:2956–2960.
5. Hollander D, Vadheim CM, Brettholz E, Petersen GM, Delahunty T, Rotter JI. Increased intestinal permeability in patients with Crohn's disease and their relatives. A possible etiologic factor. *Ann Intern Med*. 1986;105:883–885.
6. Irvine EJ, Marshall JK. Increased intestinal permeability precedes the onset of Crohn's disease in a subject with familial risk. *Gastroenterology*. 2000;119:1740–1744.
7. May GR, Sutherland SR, Meddings JB. Is small intestinal permeability really increased in relatives of patients with Crohn's disease? *Gastroenterology*. 1993;104:1627–1632.
8. Wyatt J, Vogelsang H, Hübl W, Waldhöer T, Lochs H. Intestinal permeability and the prediction of relapse in Crohn's disease. *Lancet*. 1993;341:1437–1439.
9. Sartor RB. Role of commensal enteric bacteria in the pathogenesis of immune-mediated intestinal inflammation: lessons from animal models and implications for translational research. *J Pediatr Gastroenterol Nutr*. 2005;40:S30–S31.
10. Strober W, Fuss IJ, Blumberg RS. The immunology of mucosal models of inflammation. *Annu Rev Immunol*. 2002;20:495–549.
11. Strober W. Why study animal models of IBD? *Inflamm Bowel Dis*. 2008;14:S129–S131.
12. Baert FJ, D'Haens GR, Peeters M, et al. Tumor necrosis factor alpha antibody (infliximab) therapy profoundly down-regulates the inflammation in Crohn's ileocolitis. *Gastroenterology*. 1999;116:22–28.
13. D'haens G, Van Deventer S, Van Hogezand R, et al. Endoscopic and histological healing with infliximab anti-tumor necrosis factor antibodies in Crohn's disease: a European multicenter trial. *Gastroenterol*. 1999;116:1029–1034.
14. Suenaert P, Bulteel V, Lemmens L, et al. Anti-tumor necrosis factor treatment restores the gut barrier in Crohn's disease. *Am J Gastroenterol*. 2002;97:2000–2004.
15. Targan SR, Hanauer SB, van Deventer SJ, et al. A short-term study of chimeric monoclonal antibody cA2 to tumor necrosis factor alpha for Crohn's disease. Crohn's Disease cA2 Study Group. *N Engl J Med*. 1997;337:1029–1035.
16. Söderholm JD, Olaison G, Peterson KH, et al. Augmented increase in tight junction permeability by luminal stimuli in the non-inflamed ileum of Crohn's disease. *Gut*. 2002;50:307–313.
17. Söderholm JD, Streutker C, Yang P-C, et al. Increased epithelial uptake of protein antigens in the ileum of Crohn's disease mediated by tumour necrosis factor α. *Gut*. 2004;53:1817–1824.
18. Wang F, Graham WV, Wang Y, Witkowski ED, Schwarz BT, Turner JR. Interferon-γ and tumor necrosis factor-α synergize to induce intestinal epithelial barrier dysfunction by up-regulating myosin chain kinase expression. *Am J Pathol*. 2005;166:409–419.
19. Marini M, Bamias G, Rivera-Nieves J, et al. TNF-α neutralization ameliorates the severity of murine Crohn's-like ileitis by abrogation of intestinal epithelial cell apoptosis. *Proc Natl Acad Sci USA*. 2003;100:8366–8371.
20. Okamoto R, Watanabe M. Cellular and molecular mechanisms of the epithelial repair in IBD. *Dig Dis Sci*. 2005;50:S34–S38.
21. Blois A, Srebro B, Mandalà M, Corti A, Helle KB, Serck-Hanssen G. The chromogranin A peptide vasostatin-I inhibits gap formation and signal transduction mediated by inflammatory agents in cultured bovine pulmonary and coronary arterial endothelial cells. *Regul Pept*. 2006;135:78–84.
22. Ferrero E, Scabini S, Magni E, et al. Chromogranin A protects vessels against tumor necrosis factor alpha-induced vascular leakage. *FASEB J*. 2004;18:554–556.
23. Helle KB, Corti A, Metz-Boutigue M-H, Tota B. The endocrine role for chromogranin A: a prohormone for peptides with regulatory properties. *Cell Mol Life Sci*. 2007;64:2863–2886.
24. Corti A. Chromogranin A and the tumor microenvironment. *Cell Mol Neurobiol*. 2010;30:1163–1170.
25. Corti A, Sanchez LP, Gasparri A, et al. Production and structure characterization of recombinant chromogranin A N-terminal fragments (vasostatins): evidence of dimer-monomer equilibria. *Eur J Biochem*. 1997;248:692–699.
26. Bruewer M, Luegering A, Kucharzik T, et al. Proinflammatory cytokines disrupt epithelial barrier function by apoptosis-independent mechanisms. *J Immunol*. 2003;171:6164–6172.
27. Sanders SE, Madara JL, McGuirk DK, Gelman DS, Colgan SP. Assessment of inflammatory events in epithelial permeability: a rapid screening method using fluorescein dextrans. *Epithelial Cell Biol*. 1995;4:25–34.
28. Puthenedam M, Wu F, Shetye A, Michaels A, Rhee KJ, Kwon JH. Matrilysin-1 (MMP7) cleaves galectin-3 and inhibits wound healing in intestinal epithelial cells. *Inflamm Bowel Dis*. 2011;17:260–267.
29. Paclik D, Lohse K, Wiedenmann B, Dignass AU, Sturm A. Galectin-2 and -4, but not galectin-1, promote intestinal epithelial wound healing in vitro through a TGF-beta-independent mechanism. *Inflamm Bowel Dis*. 2008;14:1366–1372.
30. Ceconi C, Ferrari R, Bachetti T, et al. Chromogranin A in heart failure. A novel neurohumoral factor and a predictor for mortality. *Eur Heart J*. 2002;23:967–974.
31. Pieroni M, Corti A, Tota B, et al. Myocardial production of chromogranin A in human heart: a new regulatory peptide with cardiac function. *Eur Heart J*. 2007;28:1117–1127.
32. Ratti S, Curnis F, Longhi R, et al. Structure-activity relationships of chromogranin A in cell adhesion. *J Biol Chem*. 2000;275:29257–29263.
33. Corti A, Longhi R, Gasparri A, Chen F, Pelagi M, Siccardi AG. Antigenic regions of human chromogranin A and their topographic relationships with structural/functional domains. *Eur J Biochem*. 1996;235:275–280.

34. Wirtz S, Neufert C, Weigmann B, Neurath MF. Chemically induced mouse models of intestinal inflammation. *Nat Protoc*. 2007;2:541–546.
35. MacDermott RP, Sanderson IR, Reinecker HC. The central role of chemokines (chemotactic cytokines) in the immunopathogenesis of ulcerative colitis and Crohn's disease. *Inflamm Bowel Dis*. 1998;4:54–67.
36. Sakata A, Yasuda K, Ochiai T, et al. Inhibition of lipopolysaccharide-induced release of interleukin-8 from intestinal epithelial cells by SMA, a novel inhibitor of sphingomyelinase and its therapeutic effect on dextran sulphate sodium-induced colitis in mice. *Cell Immunol*. 2007;245:24–31.
37. van Deventer SJ. Review article Chemokine production by intestinal epithelial cells: a therapeutic target in inflammatory bowel disease? *Aliment Pharmacol Ther*. 1997;11:S116–S120.
38. Poritz LS, Garver KI, Green C, Fitzpatrick L, Ruggiero F, Koltun WA. Loss of the tight junction protein ZO.1 in dextran sulfate sodium induced colitis. *J Surg Res*. 2007;140:12–19.
39. Vetrano S, Rescigno M, Cera MR, et al. Unique role of junctional adhesion molecule-a in maintaining mucosal homeostasis in inflammatory bowel disease. *Gastroenterology*. 2008;135:173–184.
40. Colombo B, Longhi R, Marinzi C, et al. Cleavage of chromogranin A N-terminal domain by plasmin provides a new mechanism for regulating cell adhesion. *J Biol Chem*. 2002; 277:45911–45919.
41. Guimbaud R, Bertrand V, Chauvelot-Moachon L, et al. Network of inflammatory cytokines and correlation with disease activity in ulcerative colitis. *Am J Gastroenterol*. 1998;93:2397–2404.
42. Arijs I, De Hertogh G, Machiels K, et al. Mucosal gene expression of cell adhesion molecules, chemokines, and chemokine receptors in patients with inflammatory bowel disease before and after infliximab treatment. *Am J Gastroenterol*. 2011;106: 748–761.
43. Aldhous MC, Noble CL, Satsangi J. Dysregulation of human beta-defensin-2 protein in inflammatory bowel disease. *PLoS One*. 2009;4:e6285.
44. Gitter AH, Wullstein F, Fromm M, Schulzke JD. Epithelial barrier defects in ulcerative colitis: characterization and quantification by electrophysiological imaging. *Gastroenterol*. 2001;121: 1320–1328.
45. Gasparri A, Sidoli A, Sanchez LP, et al. Chromogranin A fragments modulate cell adhesion. Identification and characterization of a pro-adhesive domain. *J Biol Chem*. 1997;272:20835–20843.
46. Colombo F, Curnis C, Foglieni A, et al. Chromogranin A expression in neoplastic cells affects tumor growth and morphogenesis in mouse models. *Cancer Res*. 2002;62:941–946.
47. Zhang XY, De Meester I, Lambeir AM, et al. Study of the enzymatic degradation of vasostatin I and II and their precursor chromogranin A by dipeptidyl peptidase IV using high-performance liquid chromatography/electrospray mass spectrometry. *J Mass Spectrom*. 1999;34:255–263.
48. Clemente MG, De Virgiliis S, Kang JS, et al. Early effects of gliadin on enterocyte intracellular signalling involved in intestinal barrier function. *Gut*. 2003;52:218–223.
49. Drago S, El Asmar R, Di Pierro M, et al. Gliadin, zonulin and gut permeability: effects on celiac and non-celiac intestinal mucosa and intestinal cell lines. *Scand J Gastroenterol*. 2006;41:408–419.
50. Paterson BM, Lammers KM, Arrieta MC, Fasano A, Meddings JB. The safety, tolerance, pharmacokinetic and pharmacodynamic effects of single doses of AT-1001 in coeliac disease subjects: a proof of concept study. *Aliment Pharmacol Ther*. 2007;26:757–766.